Telematics data for geospatial and temporal mapping of urban mobility: New insights into travel characteristics and vehicle specific power

Ghaffarpasand, Omid; Pope, Francis D.

DOI:
10.1016/j.jtrangeo.2024.103815

Document Version
Publisher's PDF, also known as Version of record

Citation for published version (Harvard):
Ghaffarpasand, O & Pope, FD 2024, 'Telematics data for geospatial and temporal mapping of urban mobility: New insights into travel characteristics and vehicle specific power', *Journal of Transport Geography*, vol. 115, 103815. https://doi.org/10.1016/j.jtrangeo.2024.103815

Journal of Transport Geography 115 (2024) 103815

Contents lists available at ScienceDirect

Journal of Transport Geography

journal homepage: www.elsevier.com/locate/jtrangeo

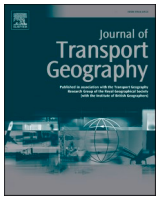

Telematics data for geospatial and temporal mapping of urban mobility: New insights into travel characteristics and vehicle specific power

Omid Ghaffarpasand, Francis D. Pope *

School of Geography, Earth, and Environmental Sciences, University of Birmingham, Birmingham, UK

ARTICLE INFO

Keywords:
Telematics data
Road transport
Vehicle specific power
Urban mobility

ABSTRACT

This paper describes a new approach for understanding urban mobility called geospatial and temporal (GeoST) mapping, which translates telematics (location) data into travel characteristics. The approach provides the speed-acceleration profile of transport flow at high spatial and temporal resolution. The speed-acceleration profiles can be converted to vehicle-specific power (VSP), which can be used to estimate vehicle emissions. The underlying data used in the model is retrieved from a large telematics dataset, which was collected from GPS-connected vehicles during their journeys over the UK's West Midlands region road network for the years 2016 and 2018. Single journey telematics data were geospatially aggregated and then distributed over GeoST-segments. In total, approximately 354,000 GeoST-segments, covering over 17,700 km of roads over 35 timeslots are parameterized. GeoST mapping of the average vehicle speed (traffic flow), and VSP over different road types are analysed. The role of road slope upon VSP is estimated for every GeoST-segment through knowledge of the elevation of the start and end points of the segments. Previously, road slope and its effect upon VSP have been typically ignored in transport and urban planning studies. A series of case studies are presented that highlight the power of the new approach over differing spatial and temporal scales. For example, results show that the total vehicle fleet moved faster by an average of 3% in 2016 compared to 2018. The studied roads at weekends are shown to be less safe, compared to weekdays, because of lower adherence to speed limits. By including road slope in VSP calculations, the annually averaged VSP results differ by +12.6%, +14.3%, and + 12.7% for motorways, primary roads, and secondary roads, respectively, when compared to calculations that ignore road slope.

1. Introduction

Road transport is the backbone of the global economy, development, and prosperity, with over 1.4 billion road vehicles currently in use. Less positively, road transport is one of the leading global sources of air pollution and accidents. For example in the EU, approximately 28% of the total nitrogen oxides ($NO_x = NO + NO_2$) emissions are attributed to the transportation sector in 2018 (EEA, 2019). In 2016, over 7.9 million tonnes CO_2 emissions were registered for road transport across the globe (21% of total global emissions), and so it is also a major source of greenhouse gas and hence climate change (IEA, 2020).

Various abatement strategies have been established across the globe to mitigate environmental and health drawbacks of the transportation sector, while simultaneously optimizing economic and developmental benefits. The implementation of low emission zones (LEZs) and the establishment of emission regulations are examples of such strategies to mitigate on-road emissions, see for example (Börjesson et al., 2021; Osei et al., 2021; Pestel and Wozny, 2021). A deep understanding of urban mobility and road transport is a prerequisite for all those strategies and approaches (Ghaffarpasand et al., 2024). If available, this data could also be exploited for other urban and transport planning purposes. The essential need for 'big data' approaches for the modelling and planning of transport systems was discussed by previous investigators such as (Milne and Watling, 2019). Intelligent transport systems (ITS), which are proposed to control traffic flow and reduce congestion in urban environments, require detailed data about urban mobility over the street network (Javed et al., 2019). The application of almost all of the new advanced technologies such as Vehicle to Vehicle (V2V) communications, Internet of Things (IoT), and Internet of Vehicles (IoV) in urban transport is strongly linked to such a deep understanding of urban mobility, see for example (Wu et al., 2021).

Before the civilian availability of geographic positioning systems (GPS), road data were primarily generated using test or traced vehicles (Mcfarland, 1956; Michon and Koutstaal, 1969). After the wide global

* Corresponding author.
E-mail address: f.pope@bham.ac.uk (F.D. Pope).

https://doi.org/10.1016/j.jtrangeo.2024.103815
Received 31 October 2022; Received in revised form 18 December 2023; Accepted 1 February 2024
Available online 13 February 2024

access to GPS and the advancements in computational processing capabilities, the breadth and depth of the information extracted from roads were hugely extended; the transport applications of data collected from GPS-connected vehicles have been evidenced by a wide body of research. For example, (Necula, 2015) applies a statistical approach on data collected from 10,000 GPS-connected vehicles to extract outlier traffic patterns. (Tang et al., 2015) used the data of >1100 taxis in the city of Harbin, China, to analyse human mobility across the studied area using the estimated average speed. (Gately et al., 2017) use GPS data of in-vehicle mobile phones and onboard navigation systems to study vehicle emissions across the metropolitan area surrounding Boston, Massachusetts, US. They used GPS data to quantify hourly vehicle average speeds over 67,000 segments across the domain. The corresponding speed-based emission factors (EFs) for every segment were then extracted from the EPA Motor Vehicle Emission Simulator (MOVES). (Ibarra-Espinosa et al., 2020) use the data collected from the GPS-connected vehicles moving over the city of Sao Paolo, Brazil, to develop vehicular emission inventory with high spatial and temporal resolutions, where they used GPS records and the Vehicular Emission Inventory (VEIN) model to estimate traffic flow information and then model vehicle emissions accordingly.

The published studies that use GPS data of vehicles already provide a detailed spatial understanding of the average speed of traffic flow over the roads. Similarly, satellite navigation (SatNav) services such as GoogleMap, Waze, etc., provide detailed spatial and temporal information on traffic routing that can estimate travel and arrival times that consider characteristics such as shortest distances, avoiding motorways, and avoiding tolls. They achieve this through the calculation of average speeds along connected links between pairs of destinations as well as using traffic forecasts, incident reports and other cognate information. However, existing studies and services do not deliver a detailed picture of the speed-acceleration-variation profile of the roads (road dynamics), hence they cannot determine real-world emissions and energy consumption patterns. Moreover, satnav services are typically only online and in real-time, so it is difficult to access and analyse their historical data, which precludes their use in transport planning and decision-making.

National emission inventories (NEI) for vehicle emissions typically develop emission factors (EFs) which are related to the annual average speed over every link of the city. For example, NEI in over 22 European member states is developed using the vehicle emission model of COPERT (COmputer Programme to calculate Emissions from Road Transport) which provides a detailed list of speed-based EFs (Dey et al., 2019). Recent sensitivity and technical analyses show significant uncertainties for speed-based emission factors (EFs) and strongly advise using speed-acceleration-based EFs instead (Dey et al., 2019; Kioutsioukis et al., 2010). Some vehicle emission models, such as International Vehicle Emissions (IVE), use vehicle-specific power (VSP) to estimate EFs, see for example (Ghaffarpasand et al., 2021b). VSP is a highly informative metric for the study of vehicle emission and fuel consumption trends, which is estimated through the speed-acceleration-variation profile (Jimenez-Palacios, 1998). All techniques, methods, and services mentioned above which have been working with vehicle float data are not able to provide a detailed picture of speed-acceleration-variation profile over the roads.

The development of driving cycles (DCs) is an attempt to deepen our understanding of the speed-acceleration-variation profile over urban environments. DCs are primarily designed to analyse typical journey patterns and extents of operation for different transport modes (Ghaffarpasand et al., 2021b; Frey and Zheng, 2002; Nam, 2009). DCs, which support the compliance testing of road vehicles, provide speed-time patterns to represent the driving behaviour of a population of vehicles within a study area (Galgamuwa et al., 2015; Lyons et al., 1986; Tong and Hung, 2010). However, the spatial and temporal representativeness of DCs beyond their study areas has been seriously queried (Ghaffarpasand et al., 2021a; Pouresmaeili et al., 2018). DCs provide an annual overview of transport within a city-scale resolution. They do not capture the full complexity and dynamics of urban mobility due to the lack of adequate spatial and temporal road data during their development. The DCs are typically developed using data from a limited number of test vehicles travelling on the roads.

Telematics data is a valuable resource for transport research as it can help address the shortage of road data mentioned above. However, its full potential has not been adequately explored (Gao et al., 2022). Telematics data refers to GPS data collected from vehicles for specific purposes, such as insurance, freight transport, and improving Intelligent Transport Systems (ITS) credibility. The primary source of telematics data within urban environments is the GPS-connected vehicles, whose drivers would like to enjoy fairer insurance premia and so voluntarily share their location data with the insurance companies. The research studies in the literature predominantly use telematics data to investigate driving behaviour (Xiang et al., 2024). For example (Huang and Meng, 2019) investigated the use of extensive driving behaviour characteristics extracted from telematics data in predicting the risk probability of insured vehicles. (Ziakopoulos et al., 2022) investigated the role of telematics data in road safety and found a reduction of 20–43% in car crashes. (Alrassy et al., 2023) used telematics data of 4500 light-duty vehicles to analyse the driving behaviour within New York, US. Their method was unable to deliver a temporal picture of urban mobility. While valuable research has explored the wide applications of telematics data in road safety and driving behaviour analyses, a universal approach to translating telematics data into road dynamics in terms of the speed-acceleration-variation profile of the roads has not been developed until this study.

This study develops a new approach to understanding and parameterizing urban mobility, road dynamics and road transport via geospatial and temporal mapping. We used a large telematics dataset to determine the travel characteristics of the whole West Midlands region of the UK. Using this data, we exemplify the approach by investigating the temporal variation of vehicle fleet speed over different geospatial scales, from a single road segment to the whole of the West Midlands region. We compare the outputs from the approach with other traffic flow datasets. Finally, we provide an example of how the speed and location derived from telematics can be used to generate estimates of fleet-averaged VSP from which fuel consumption and air pollutant emission estimates can be derived (Ghaffarpasand and Pope, 2023). It is noted that to generate fuel consumption and emissions estimates further information is required, including fleet composition, and emission factor datasets. These datasets are not presented in this paper. This paper provides a new methodology for obtaining road segment and temporally aggregated road dynamics, including VSP, from telematics data.

The paper is structured as follows: the next section details the materials and methods used. Section 3 assesses the results of this study against figures provided by local transport organizations. Section 4 provides the results and discussions, while Section 5 outlines the major take-home messages of the paper.

2. Material and methods

2.1. Telematics data

The telematics data was obtained from The Floow, a UK-based telematics company (www.thefloow.com), which sampled a fraction of the light-duty vehicle (LDV) fleet in the West Midlands region of the UK. Telematics data is usually collected by various devices such as black boxes, onboard diagnostic (OBD) devices, 12 V plugin devices, original equipment manufacturer (OEM) devices, tachographs, and driver smartphones (Ghaffarpasand et al., 2022). The predominant contribution data used in this study was collected from the OBDs. The sample vehicles in the fleet are GPS-connected passenger cars, in which the drivers share their driving data to reduce the cost of their insurance premia. It is estimated that approximately 3–7% of the total on-road

fleet provides the telematics data in this study, with the exact percentage depending on the time and place of the data sampling.

The instantaneous speed-time data of the individual vehicles were measured using the doppler-aided positioning method. A schematic diagram of the doppler-aided positioning technique is provided in Fig. 1. Global navigation satellite systems (GNSS) allow for two techniques of precise point positioning (PPP) and real-time kinematics (RTK), which were developed for precise positioning and navigation. RTK can achieve high accuracy positioning, on the order of cm, with quick convergence in real-time monitoring and post-monitoring analysis. Doppler-aided positioning significantly improves single-frequency RTK in urban environments (Bahrami and Marek, 2010). GPS and other GNSS usually use the doppler shift of the received carrier frequencies to determine the speed of a moving object. The instantaneous speed-time data used in the current study were measured using the doppler-aided positioning method. The corresponding instantaneous accelerations are then calculated using the temporal variation of speed.

The instantaneous speed-acceleration-time telematics data are collected from the individual GPS-connected vehicles for their journeys over road segments providing the raw material for the current study. A journey is a time series of telematics data and so the concepts of 'journey' and 'telematics data' are interchangeably used in this study. The individual vehicle telematics data are firstly QC/QA checked by the company (The Floow). The company is not allowed to deliver the data of individual vehicles because of the General Data Protection Regulation (GDPR) in the EU and UK. Hence, they anonymized and then aggregated the data by road segment and time bins. After aggregation, every road segment contains the average collection of all journeys (speed-acceleration-time data) for certain time bins.

The studied street network is quantized into segments as geographic polylines with known start and end points. The segments cover all features of the studied road network, with segment lengths varying between approximately 15 and 150 m. Segments are used to approximate straight and curved sections and distinct road features such as roundabouts, junctions, etc. Segments have a spatial identity complemented by a temporal identity, in addition to having a direction, so henceforth they are named GeoST (geospatial and temporal) segments.

The aggregated journeys are subset over GeoST segments, and a speed-acceleration-frequency-distribution (SAFD) matrix is calculated for every GeoST-segment. SAFD of the GeoST-segments were delivered by the telematics company. SAFD is a normalized matrix representing the distribution of the instantaneous speeds and accelerations over every GeoST-segment; an example of SAFD for a typical GeoST-segment is shown in Table 1. Here, for example, the shaded element indicates that 7.78% of journeys in the studied GeoST-segment have speed and acceleration within the ranges of 16-18 m/s and -1-0 m/s^2 respectively. SAFDs have previously been used to develop driving cycles and within the literature, there are different selections of bin properties for the classification of speed and acceleration, see for example (Huertas et al., 2018; Yuhui et al., 2019).

With the speed and acceleration divisions presented in Table 1, SAFD is an 18×10 matrix which provides the frequency distribution across the combination of 18 speeds and 10 acceleration bands. The average speed and acceleration of each GeoST-segment are calculated by the following equations:

$$\bar{v} = \sum_{i=1}^{18} \sum_{j=1}^{10} \left[[SAFD]_{18\times10} \times [v_{median}]_{18\times10} \right]_{i,j} \quad (2)$$

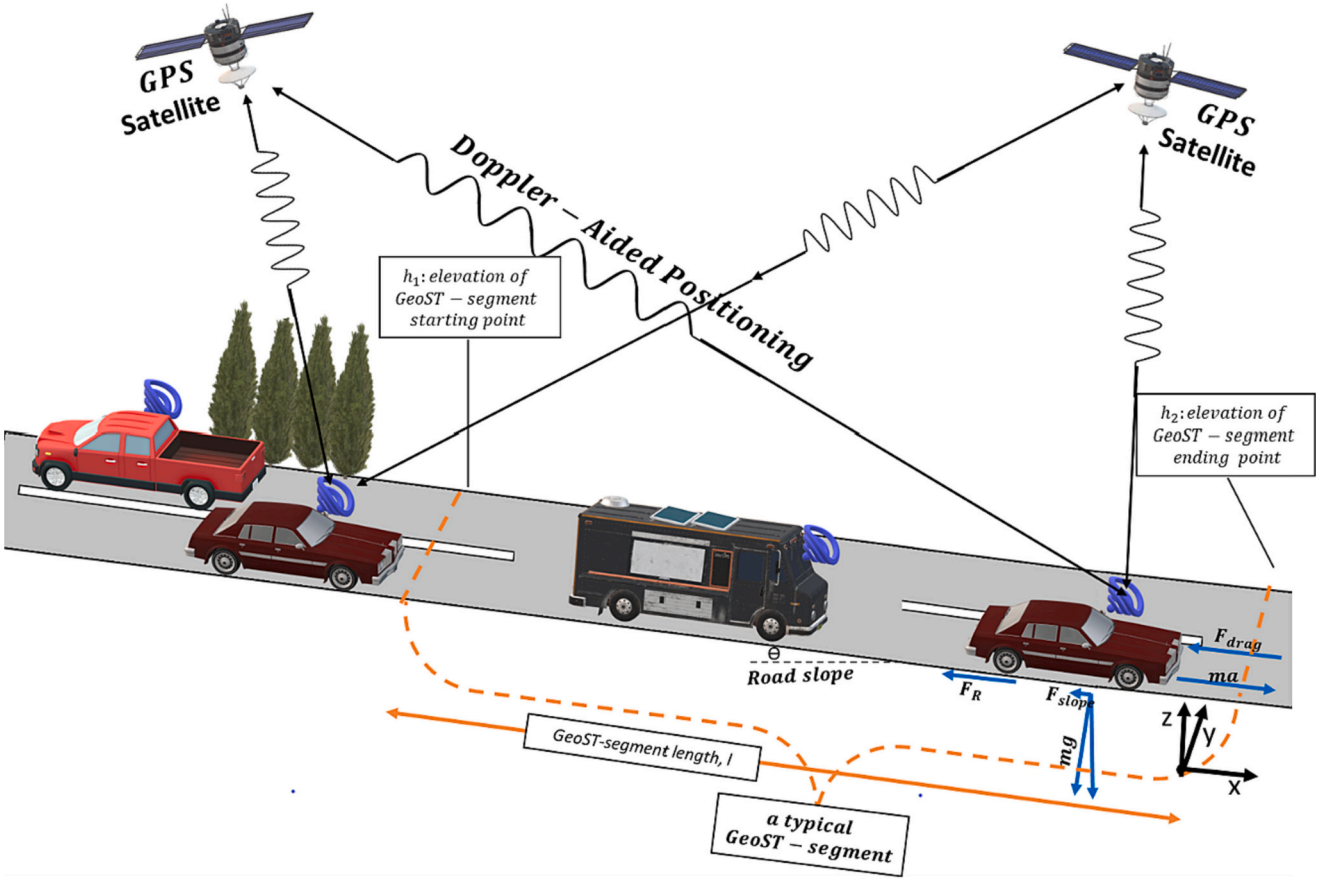

Fig. 1. A schematic diagram of different elements in GeoST mapping of urban transport/mobility including connected vehicles to the GPS satellites, the Doppler-aided positioning technique for estimating the instantaneous vehicle speed, a typical GeoST segment, and a diagram of the exerted forces on a typical vehicle.

Table 1
The speed-acceleration-frequency-distribution (SAFD) matric (in %) of a typical GeoST-segment averaged over the whole of 2018.

		Acceleration (m/s^2)									
		< −4	−4 − 3	-3 − 2	-2 − 1	-1-0	0–1	1–2	2–3	3–4	4 <
	0–2	0.00	0.00	0.00	0.00	0.00	0.00	0.00	0.00	0.00	0.00
	2–4	0.00	0.00	0.00	0.16	4.86	6.77	0.97	0.16	0.00	0.00
	4–6	0.00	0.00	0.07	0.62	2.71	2.44	0.80	0.11	0.00	0.02
	6–8	0.00	0.01	0.15	0.73	2.91	2.99	0.63	0.02	0.00	0.00
	8–10	0.00	0.02	0.16	0.73	2.89	2.25	0.40	0.02	0.00	0.00
	10–12	0.01	0.01	0.15	0.71	3.92	2.32	0.19	0.05	0.00	0.00
	12–14	0.00	0.01	0.13	0.77	7.06	4.07	0.50	0.02	0.00	0.00
	14–16	0.01	0.02	0.09	0.52	8.94	6.15	0.30	0.01	0.50	0.00
	16–18	0.00	0.01	0.03	0.40	7.78	5.91	0.45	0.01	0.00	0.00
	18–20	0.00	0.01	0.03	0.17	4.10	2.94	0.40	0.01	0.00	0.00
	20–22	0.00	0.01	0.01	0.20	2.31	1.08	0.40	0.30	0.00	0.00
	22–24	0.00	0.01	0.01	0.20	0.39	0.44	0.01	0.30	0.00	0.00
	24–26	0.00	0.01	0.01	0.30	0.27	0.06	0.02	0.01	0.00	0.00
	26–28	0.00	0.01	0.01	0.40	0.24	0.04	0.40	0.01	0.00	0.00
	28–30	0.00	0.00	0.01	0.01	0.21	0.02	0.00	0.00	0.00	0.00
	30–32	0.00	0.00	0.00	0.01	0.01	0.01	0.01	0.01	0.00	0.00
	32–34	0.00	0.00	0.00	0.00	0.00	0.00	0.00	0.00	0.00	0.00
Speed (m/s)	***> 36***	0.00	0.00	0.00	0.00	0.00	0.00	0.00	0.00	0.00	0.00

$$\bar{a} = \sum_{i=1}^{18}\sum_{j=1}^{10}\left[[SAFD]_{18\times10} \times [a_{median}]_{18\times10}\right]_{i,j} \quad (3)$$

where $\bar{v}$, $\bar{a}$, $[SAFD]_{18\times10}$, $[v_{median}]_{18\times10}$, and $[a_{median}]_{18\times10}$ are the average speed (m/s), the average acceleration (m/s^2), SAFD matrix, the median speed matrix and the median acceleration matrix, respectively. Median speed and acceleration matrices are produced using the corresponding median values of speed and acceleration ranges for every element of the SAFD matrix. Travel time (t) of every GeoST segment for each time slot can be calculated by: $t = l/\bar{v}$, where l is the segment length.

2.2. Segment-based estimation of vehicle-specific power (VSP)

The approach proposed here can provide a detailed picture of VSP spatiotemporal distribution over the roads. VSP was first used by (Jimenez-Palacios, 1998) as the vehicle power demand at a particular point to overcome the external forces, including inertial forces to keep acceleration a ($F_{inertial} = ma$), resistance force caused by the road friction (F_R), air resistance drag (F_{drag}), and road slope force (F_{slope}), imposed on a moving vehicle, as represented in Fig. 1. Accordingly, power demands for a vehicle at constant speed include the power to accelerate the vehicle (P_{acc}), to overcome rolling resistance from the road (P_{roll}), to overcome air resistance (P_{air}), to overcome road slope force (P_{grad}), and to operate auxiliary devices (P_{aux}). P_{trans} should be also considered as the power losses in the transmission. The following equation is proposed as the total power demand (in W):

$$P_{tot} = P_{acc} + P_{roll} + P_{air} + P_{grad} + P_{aux} + P_{trans} = \left[m \times a \times 1.04 + R_0 + R_1 \times v + 0.5 \times C_d \times A \times \rho \times v^2 + m \times g \times Grad\right] \times 1.08 \times v + 2500 \quad (4)$$

where m, a, v, C_d, and A are vehicle mass (t), vehicle acceleration (m/s^2), vehicle speed (m/s), aerodynamic drag coefficient, and frontal surface area (m^2), respectively. R_0(N) and R_1(N/(m/s)) are road load coefficients. g and ρ as the gravity and air density are assumed as $9.81 m/s^2$ and $1.2 kg/m^3$ in the ambient temperature of 20 °C and the atmospheric pressure of 1 atm. *Grad* stands for road slope and will be discussed in the sections ahead. To arrive at the equation above, a few assumptions are required (Davison et al., 2020). First, it is assumed that 4% of the power for translational mass is consumed to accelerate rotational accelerated mass. Also, 8% of the power at the driven wheel losses during transformation. Finally, the fixed value of 2.5kW is the power demand of auxiliaries. Under these assumptions and for passenger cars, *VSP* as the required power per mass ($VSP = P_{tot}/m$) is given by:

$$VSP = v \times \left(1.1 \times a + \overbrace{(9.81 \times Grad + 0.132)}^{slope\ part}\right) + 0.00302 \times v^3 \quad (5)$$

A VSP based matrix ($[VSP\ matrix]_{18\times10}$) is calculated for which every element is estimated by the equation above and corresponding median values of speed and acceleration (see Eqs. (2) & (3)). The VSP of every segment is then calculated by the following equation:

$$VSP_{seg} = \sum_{i=1}^{18}\sum_{j=1}^{10}\left[[SAFD]_{18\times10} \times [VSP\ matrix]_{18\times10}\right]_{i,j} \quad (6)$$

(Davison et al., 2020) found an acceptable agreement between the vehicle emissions modelled by the VSP equation and real-world emission measurements. VSP plays a vital role in translating the driving dynamics into the transport environment dimensions such as fuel consumption and exhaustive emissions, see for example (Grange et al., 2019). In most of the literature, however, the slope part in Eq. (5) is ignored. To discuss the role of road slope in urban mobility characteristics, two VSP_{seg} values are estimated for every GeoST-segment, one in which includes the slope part of Eq. (5), and one where the influence of slope is ignored.

2.3. Spatial and temporal scope of the study

The street network of the West Midlands in the UK (Fig. 2(a)) is the spatial scope of the present study. The West Midlands is one of the nine official regions of England in Great Britain. It contains 27 constituencies (Fig. 2(b)) and seven main boroughs including Birmingham, Coventry, Wolverhampton, Dudley, Sandwell, Solihull, and Walsall which are distinguished by different colours in Fig. 2(c). The population of the West Midlands was around three million inhabitants in 2020. Using the segment-based method discussed in Section 2.1, the West Midlands street network is subdivided into 353,579 GeoST segments which cover 17,745 km (around 4.5% of England's road length); 398,312 km is the

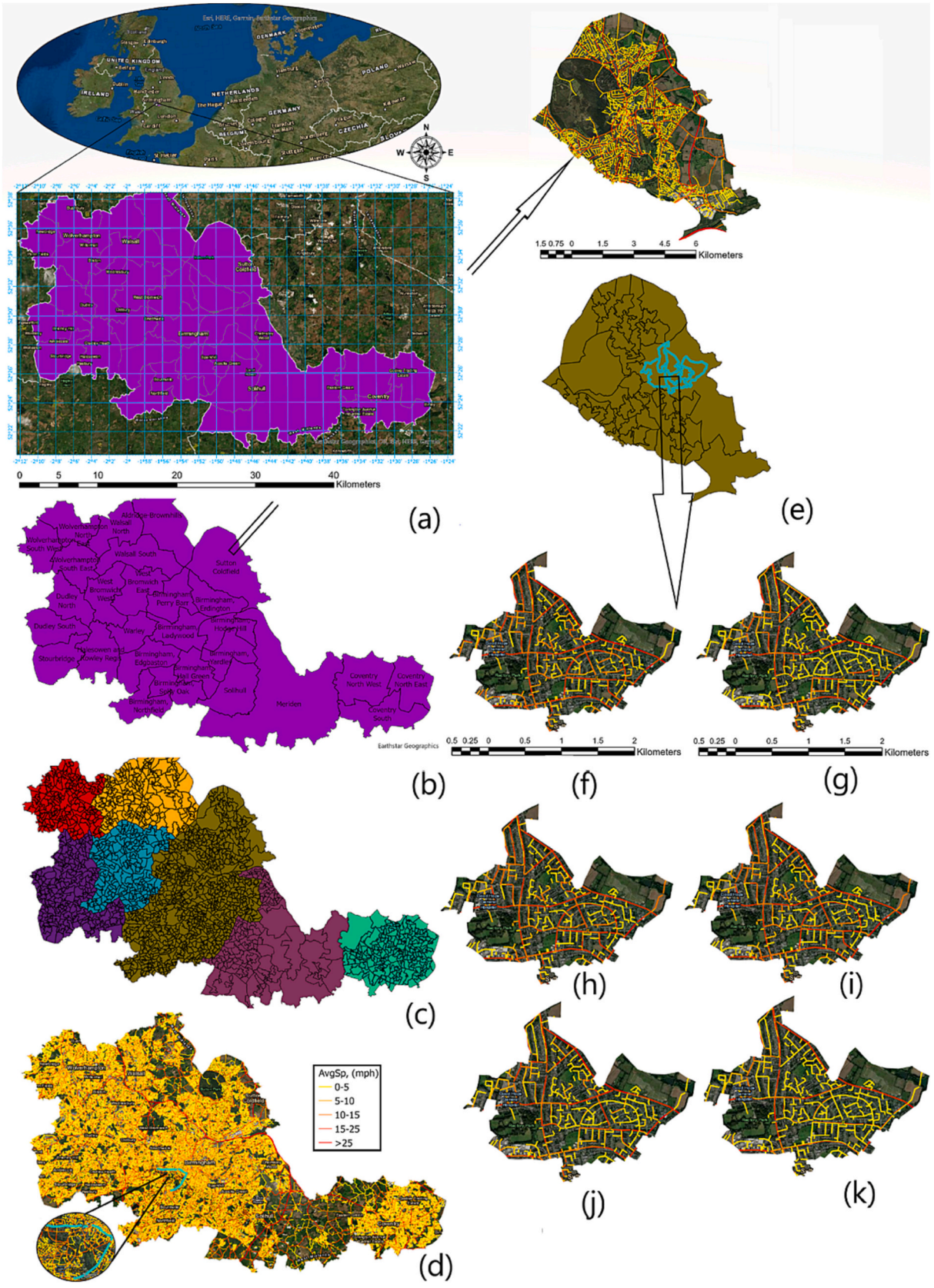

Fig. 2. (a) West Midlands as the scope of the current study; (b) 27 constituencies of the West Midlands; (c) LSOAs in the West Midlands; (d) annual average speed over West Midlands street network; (e) annual average speed over the street of Sutton Coldfield, one of the West Midlands constituencies; annual average speed over the streets of three LSOAs of Sutton Coldfield for Mondays (f) 07:00–08:59, (g) 09:00–11:59, (h) 12:00–13:59, (i) 14:00–16:59, (j) 16:00–18:59, and (k) 19:00–23:59.

total road length of England (DFT, 2020; DFT, 2022). We follow the standard national guidelines for mapping roads in the United Kingdom (UK) proposed in OpenStreetMap (https://wiki.openstreetmap.org/wiki/Roads_in_the_United_Kingdom) which divide the UK roads into motorway, trunk, primary, secondary, tertiary, unclassified, residential, service, private, and track. In this study, we present the results for the motorways, primary, and secondary roads of the West Midlands.

The West Midlands telematics dataset is generated for two whole years: 2016 and 2018. These years were chosen because they represent baseline years which were not significantly affected by either planned or unplanned interventions such as the COVID-19 pandemic (2020 to present times) or the implementation of the Clean Air Zone (CAZ, 01/06/2021 to present times), respectively.

The annual data is temporally split into 35 time-slots including seven diurnal time-slots (00:00–06:59, 07:00–08:59, 09:00–11:59, 12:00–13:59, 14:00–15:59, 16:00–18:59, and 19:00–23:59) in five days (Mondays, Tuesdays, Fridays, Saturdays, and Sundays). It was assumed that the traffic behaviour on Wednesdays and Thursdays was similar to Tuesdays. The selected hours of the day were chosen to correspond to weekday 'early morning hours', 'morning rush hours', 'morning non-

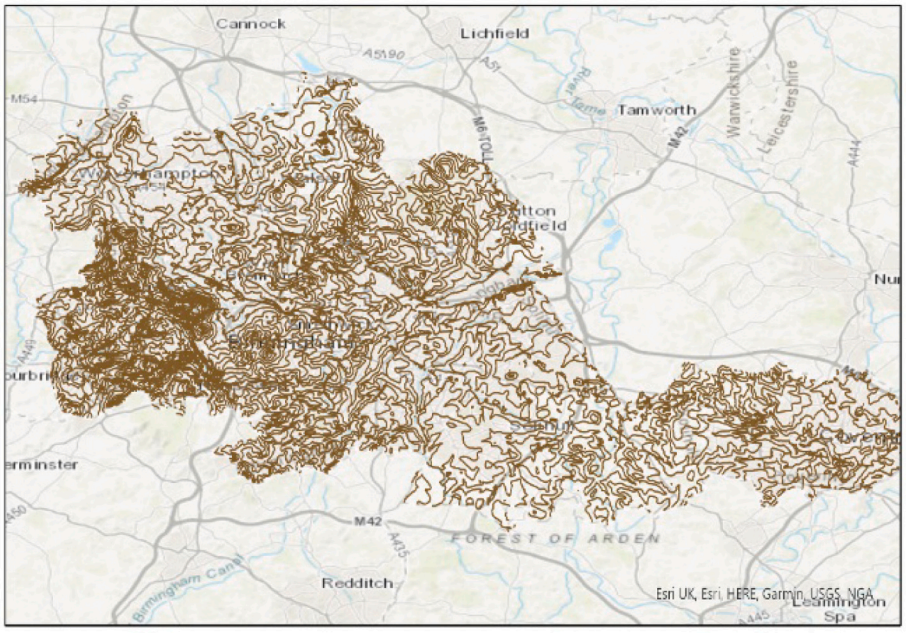

(a)

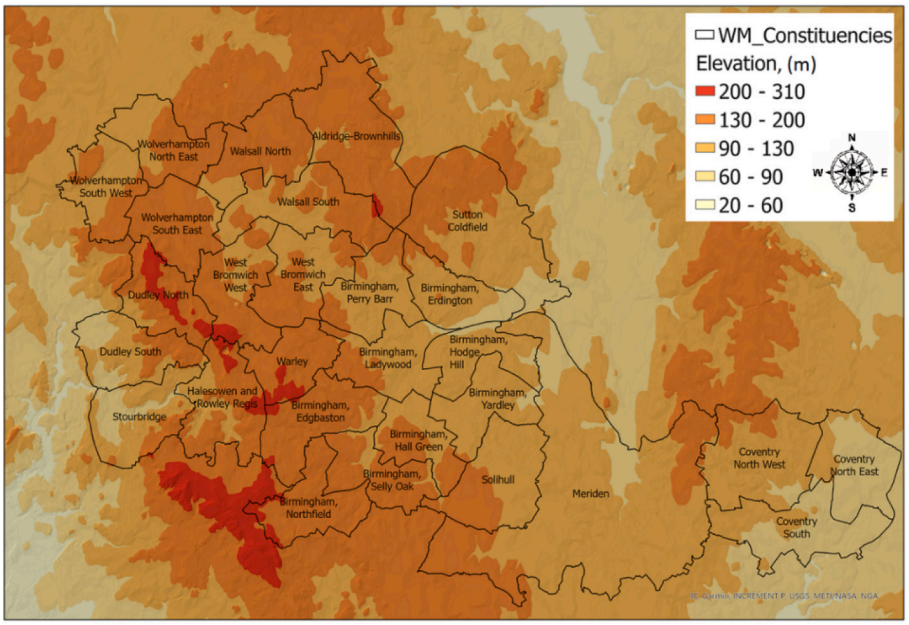

(b)

Fig. 3. (a) The elevation contour and (b) DEM of the West Midlands; (c) speed limit over a small area of the constituency of Erdington in the city of Birmingham, West Midlands, UK.

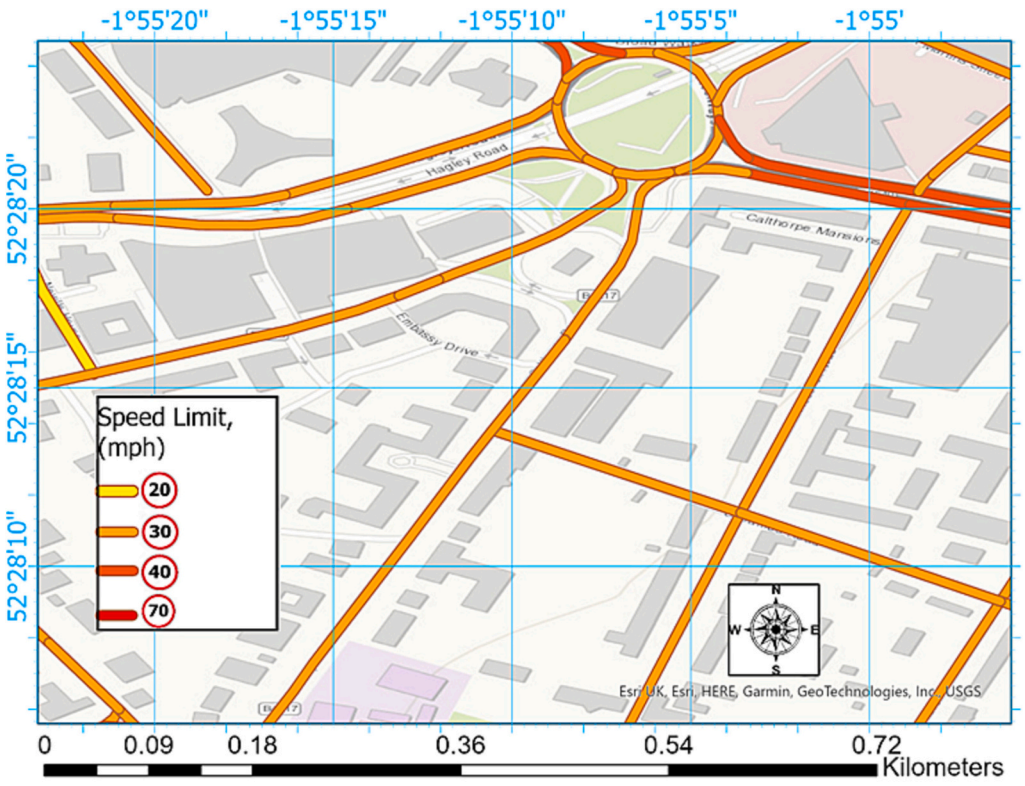

(c)

Fig. 3. (*continued*).

rush hours', 'noon rush hours', 'afternoon non-rush hours', 'evening rush hours', 'evening non-rush hours', respectively. The same descriptors are used throughout the manuscript for the different time slots even for weekends when the busy and slow periods are distinct from weekdays.

2.4. Geospatial estimation of segment slopes

Road slope is an important geospatial characteristic which affects VSP and hence emissions, see Eq. (5), which has been ignored in most of the transport and urban planning studies. Road slope is calculated through knowledge of elevation variation and the length of the road segment. The open elevation contour lines for West Midlands are downloaded from Ordnance Survey (OS), through www.ordnancesurvey.co.uk, the national mapping agency of the UK. OS provides the most accurate and up-to-date geographic data, relied on by local authorities, businesses and individuals; the standard errors for OS Net base station coordinates are generally better than 0.008 m in plan and 0.020 m in height. The elevation contour map of the West Midlands is given in Fig. 3(a). Using ArcGIS Pro 2.8.2, the elevation contours are converted into a digital elevation model (DEM). The DEM for the West Midlands is shown in Fig. 3(b). The inverse distance weighted (IDW) technique is applied to interpolate the elevation values for the unknown points. As shown in Fig. 1, each GeoST-segment is determined by a pair of start and end points. Hence, two point-layers including the location of starting and ending points are produced and the incorporated elevations are estimated using the DEM for the West Midlands, and the tool *Extract Values to Points* from *Spatial Analyst* section of ArcGIS Pro. The segment slope is then calculated by the following equation

$$Grade\ (Road\ Slope) = \frac{h_2 - h_1}{l} \tag{7}$$

where h_1, h_2 and l are the elevations of the start and end points, and the segment length, respectively. The start and end points are defined with respect to the direction of the traffic flow, whereby a pair of GeoST-segments are determined for every piece of the considered roads. Most of the existing traffic flow models provide singular values for the vast majority of road networks, i.e., they do not differentiate between the direction of travel on the same road. The calculation of road slope is reliant on the heights and the end points of a segment, and it is theoretically possible that multiple slopes could exist within individual gradients. However, the West Midlands is not a particularly hilly area, and the estimated mean (positive) road slope is 0.015. All the GeoST segments have lengths smaller than 150 m (81% of them have lengths smaller than 100 m), and the estimate of slope is unlikely to be significantly over or under-estimated.

2.5. Speed limits over the GeoST-segments

The road speed limit provides legal guidance on what threshold speed is allowed for a given road; the threshold value is chosen to provide safety to users of the road vehicles and other users of the road and surrounding areas (Administration, F. H, 1998; DFT, 2013). A wide body of research has analysed the existing correlations between speed limits and road safety measures, see for example (Elvik, 2005; Zhai et al., 2022; Li et al., 2013). The speed limit maps of many areas around the world are widely available on the web. We use OpenStreetMap (https://www.openstreetmap.org/) to generate the speed limit map of the West Midlands. Shapefiles are downloaded from http://geofabrik.de which is the download server for the OpenStreetMap datasets. The speed limit map of a small area in the constituency of Erdington in the city of Birmingham is represented in Fig. 3(c) as an example. The speed limit map of the studied area is a GIS polyline layer. The corresponding speed limit of

every GeoST-segments is determined by the consecutive use of Buffer and spatial join tools in the ArcGIS Pro. The method is discussed in more detail in the next section. The number of GeoST segments whose average speed exceeds the corresponding speed limit to the total number of GeoST segments is introduced as the percentage of the segments with average speed exceeding the speed limit.

As discussed earlier, GeoST-segments contain aggregated data, for which the parameter "percentage of the segment with average speed exceeding the speed limit" can be considered as a proxy of relative road safety.

3. Justifications and limitations for using telematics data

Telematics data are mainly collected from the vehicles of drivers who would like to have fairer insurance premia. Hence, there is a concern that telematics enabled vehicles to drive unusually (at slower speeds and with fewer harsh accelerations) to secure their insurance discount; a manifestation of the so-called Hawthorne effect (Brannigan and Zwerman, 2001). However, it has been evidenced that the Hawthorn effect is short-lived; typically 2–4 weeks before reverting to normal behaviours meaning most tracked drivers are not influenced significantly by the tracking itself (Brannigan and Zwerman, 2001). Meanwhile, there are concerns about the spatiotemporal distribution of telematics data density as well as the credibility of the extracted statistics over the road network. The data density of telematics is much greater than most DCs, which are typically developed with the data of a few (less than five) GPS-connected vehicles which move over the roads of the studied area (Ghaffarpasand et al., 2021b; Frey and Zheng, 2002; Nam, 2009). It has been argued that the travel data of test vehicles could reflect the corresponding transport status there; the vehicles flow through the traffic stream and obey the road conditions. The same can be argued for telematics data. In this study, we had access to the data of at least 3–7% of the total on-road fleet.

Although vehicle telematics data has wide potential applications, the telematics industry is faced with some limitations. The transparency of telematics data is a major issue, particularly for online initiatives. Existing regulations, such as GDPR, enforce strict rules on data anonymisation. Despite the pace of advancements in edge computing, there is still a long way to go in terms of node anonymisation and online exploitation of telematics data. Another potential limitation is the source of telematics data. OBDs have been the primary source of data from 2010 to 2020, although the use of drivers' cell phones to collect telematics data has been increasingly considered in recent years. Combining data from multiple sources is crucial to ensure the accuracy of the results, given the use of different data collection techniques. For a detailed discussion of the challenges facing the telematics industry, please refer to the review paper written by (Ghaffarpasand et al., 2022).

4. Results and discussions

As was discussed above, the low level of spatial and temporal resolutions are the main drawbacks of the traditional transport data which cause several issues in transport planning, policy formulation and decision-making, see for example (Milne and Watling, 2019). To demonstrate the power of the new telematics-based approach introduced in this paper, we provide a series of case studies: (1) mapping travel characteristics over a variety of spatial scales, (2) comparison with other traffic model data, (3) detailed travel characteristics of single road GeoST-segments, (4) detailed travel characteristics of a set of GeoST-segments. The case studies do not just show the mapping power of the approach but also deliver new insights into the travel characteristics and microfeatures of traffic behaviour over the urban road network that hitherto have not been evidenced. Further, we study the spatiotemporal distribution of VSP over different road types and analyse the role of road slope in the VSP estimations which have been ignored in almost all published transport studies.

4.1. Mapping travel characteristics

GeoST mapping of urban mobility can translate vehicle telematics data into various travel characteristics such as average speed, average acceleration, travel time, etc., over high spatial and temporal resolutions. Here, we present the average speed of vehicles over the studied roads. The annual average speed of vehicles over the West Midlands street network is shown in Fig. 2(d). The telematics data can be used to map different spatial scales, from regional to street level. All the West Midlands LSOAs (layer super output areas) are represented in Fig. 2 (c). Fig. 2(e) provides the annual average speeds over the street network of the constituency Sutton Coldfield. The temporal variations in the annual average speed are demonstrated in Fig. 2 (f-k), where the average speed for different periods is represented.

The generated maps, which are exemplified in Fig. 2, are very useful for hotspot analysis of congestion and other travel characteristics. Such urban mobility maps can identify the spatiotemporal clustering of, for example, the percent time driving spent in the creeping condition ($\overline{v} < 5$ km/h, and $-1\ m/s^2 < \overline{a} < +1\ m/s^2$), which represents the congestion pattern over the studied area (Arun et al., 2017). Typically, pre-existing traffic models just provide annual values over much larger aggregated areas, whereby temporal analysis of congestion patterns is less useful. Satnav services also deliver an instant picture of the average speed over the studied area which could be significantly affected by temporal road constructions, car accidents, etc. Hence, they could not deliver a detailed picture of urban transport suitable for further hotspot analysis and transport planning. Hence, the approach provided here will provide a significant new data source and tool for urban and transport planners.

4.2. Comparison of telematics-derived speed with existing models

The telematics-based dataset is generated by the real-world location data collected from the real vehicles travelling on real roads, whereas traffic flow is usually characterized by numerical models complemented by a wide range of field experiments/surveys such as automatic traffic number counter, ordnance surveys, GPS data of some test vehicles, etc. (Papamichail et al., 2019). We compare here (for the first time) the results of our telematics-based approach with the existing traffic models to assess the credibility and reliability of those models. Developing traffic models is time-consuming, expensive, and requires deep technical transport knowledge.

Assessing the results of the traffic model against the telematics-based dataset is not straightforward. There are significant differences between the spatiotemporal resolution and binning of the traffic model and the telematics-based dataset. Fig. 4(a) provides the annual average speed over a small area of the Erdington constituency in the city of Birmingham for the year 2016. The data is provided by both the telematics-derived data described in this paper and the traffic model used by Birmingham City Council, which is constructed on the transport modelling software of SATURN (Simulation and Assignment of Traffic to Urban Road Networks, https://saturnsoftware2.co.uk/) (BCC, 2017).

The solid and dashed lines correspond to the traffic model and telematics-based estimations, respectively. Significant differences in terms of spatial resolutions are observed between the two data sets. Within the model, minor and secondary roads are not included, and there is just one value for every street in the city, with the direction of travel ignored. The telematics data contains nearly all major and minor roads and is bidirectional. Notwithstanding the differences in the data sources, it can be seen in Fig. 4(a) that the results estimated by both approaches are almost in the same range (similar colours).

In addition to the Birmingham City Council model, there is a regional model developed by Transport for West Midlands (TfWM), which provides data for morning and evening rush hours (07:30–09:30 and 16:00–18:00) for 2018. The morning and evening rush hours are represented as AM and PM, respectively, hereinafter for the sake of brevity.

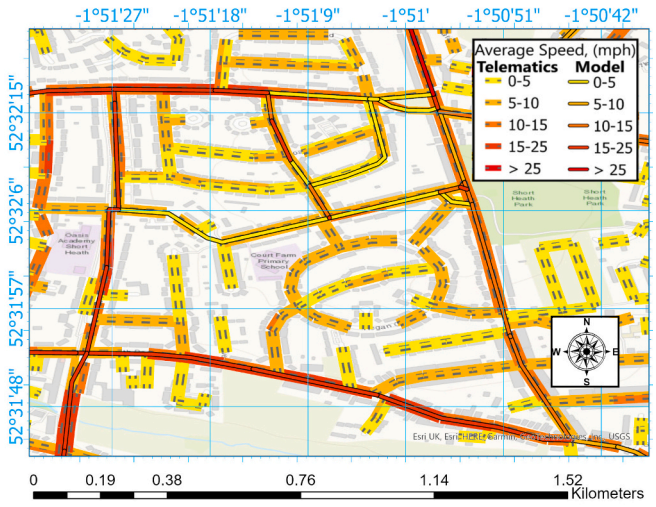

(a)

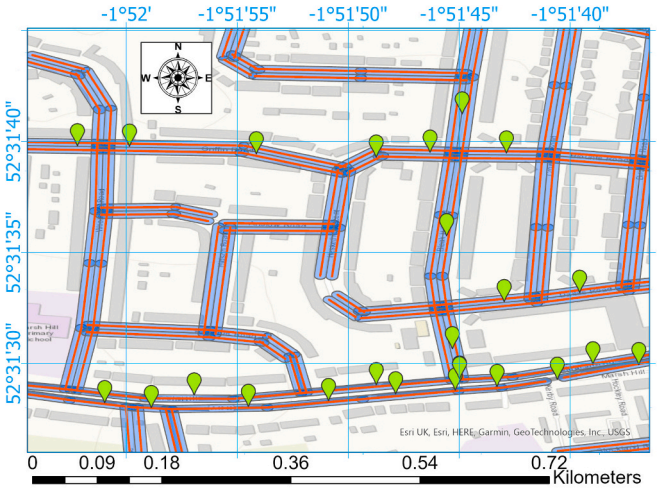

(b)

Fig. 4. (a) The annual average speed over a small area of the city of Birmingham for 2016; solid and dashed lines stand for the results of the BCC traffic flow model and this study, respectively; (b) the annual average speed over a small area of the city of Birmingham for morning rush hours in 2018; red pin markers and blue buffered polylines stand for the result of TfWM model and this study, respectively; (c) the average speed difference between the results of the TfWM model and the method proposed here. The short lines and black diamond markers denote the median and average values, respectively. AM and PM stand for the morning (07:30–09:30) and evening (16:00–18:00) rush hours, respectively. (For interpretation of the references to colour in this figure legend, the reader is referred to the web version of this article.)

Note that morning rush hour timings are offset from the definitions used in this study (07:00–08:59). There are also significant discrepancies between the spatial resolution of the two datasets with the TfWM data giving single values for many streets and ignoring the direction of traffic flow.

The TfWM data represented by the points layer correspond with 2016 AM, 2016 PM, 2018 AM, and 2018 PM for the city of Birmingham containing 18,961, 30,817, 19,210, and 29,631 points which are mainly placed on the major roads. An example of produced points layer is shown in Fig. 4(b) through green pin markers. From the telematics-based dataset, the annual average speed layers for morning and evening rush hours are calculated and reported as two polyline layers for the studied 2016 and 2018 study years and overlapped with the TfWM data. By using the *Buffer* tool in ArcGIS Pro, 10 m buffers are produced around any polylines of the considered layers. Buffered polylines are presented in Fig. 4(b) as blue rectangles. Finally, corresponding TfWM data with each buffered polyline of telematics-based results are determined using the tool *Spatial Join* in ArcGIS Pro. Two technical facts should be taken into account before analysing the results; (i) the assessment procedure is just carried out for the city of Birmingham for the years 2016 and 2018 for which the produced layers each contain 64,745 polylines covering all roads and road features of the city; (ii) the average of intersected model data is assumed as the corresponding value for telematics-based results. The average speed difference among the studied datasets is represented in Fig. 4(c) in a boxplot format, while the short lines and black diamond markers there denote the median and mean average difference values, respectively. The average speed differences for a few case studies are reported in Table 2. Despite several technical discrepancies among the datasets, the average speed differences between the two datasets are observed to be approximately 5 mph for the entire studied area and years 2016 and 2018. In motorways, however, the difference values exceed 10mph on some occasions. It is highlighted that telematics-based results are obtained by direct measurements from the roads, while TfWM (and also BCC) data is estimated

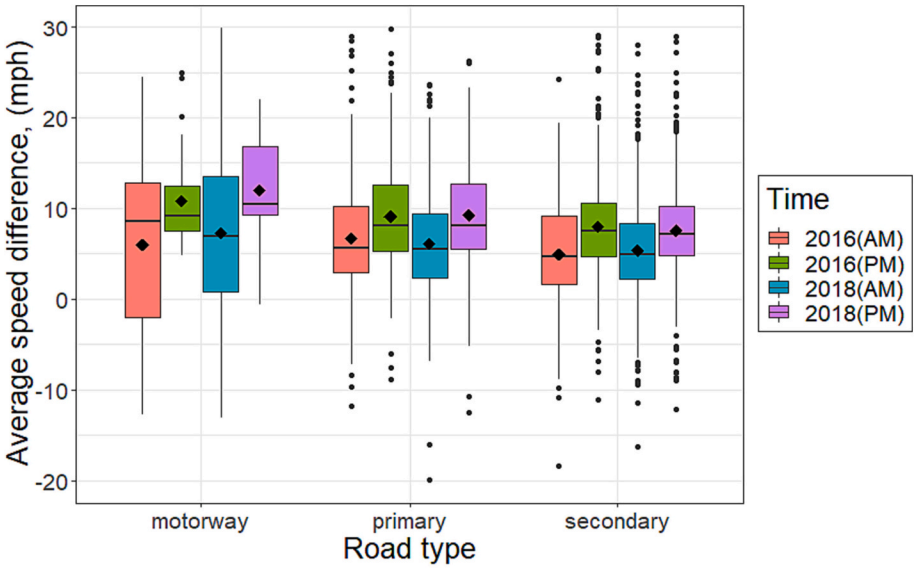

(c)

Fig. 4. (*continued*).

Table 2
The average speed differences (mph) for different case studies. AM and PM stand for the morning (07:30–09:30) and evening (16:00–18:00) rush hours, respectively.

Case	The average speed difference, (mph)
2016 AM entire West Midlands	5
2016 PM entire West Midlands	7.3
2018 AM; entire West Midlands	4.6
2018 PM entire West Midlands	5.6
Secondary roads (2016&2018)	6.6
Primary Roads (2016&2018)	7.8
Motorways (2016&2018)	10.1

by a series of models, surveys, measurements, etc.

4.3. Travel characteristics (average vehicle speed) for single road GeoST segment

In this section, we highlight the detailed information about micro-features of traffic behaviour that can be obtained for individual GeoST segments. Detailed information is necessary for planning and decision-making processes. New insights are achieved though by analysing the road transport over these small pieces of the roads, while the same spatiotemporal resolution has not been provided by previously developed methods and models. We use two crossroad GeoST segments with the same length of 150 m located near the city centre of the city of Birmingham as examples. The first segment is on the A38 and the second segment is on the A456, shown in Fig. 5(a) and (b), respectively. Both segments are bidirectional dual carriageways with data for travel characteristics in both directions. The GeoST-segment is shown in Fig. 5 (b) is next to a junction. The direction toward the Birmingham city centre is shown by a blue arrow in both figures, and the average speed in each direction, over different times of the day and days of the week (Sunday and Monday), are represented by different colours in the accompanying bar chart.

The comparison of the two road segments shows distinct temporal and directional variations in speed. Overall, the A38 segment shows faster speeds over all times when compared to the A456 segment. The A456 segment is next to a junction controlled by traffic lights, whereas the A38 segment is more distant from traffic junctions, which likely explains the overall difference in speeds between the two segments.

In general, for both segments on Monday, the average speed was slower for traffic travelling toward the city centre at all times of the day, except for the afternoon rush hour on the A38 segment. On Sunday, the average speeds for different time slices were more similar in both directions, when compared to Monday.

The slowest average speed is observed on the A38 segment on Monday for traffic travelling away from the city centre in the evening rush hour. For the A456 segment, the slowest average speed was for the morning rush hour travelling toward the city centre. One of the major benefits of GeoST mapping of urban mobility is the opportunity of conceptualizing the spatial relationships between the urban mobility characteristics and the other urban features such as schools, retail, hospitals, etc. This might be considered one of the future research directions of the current study.

4.4. Travel characteristics (average vehicle speed) for combined road segments

In this section, we analyse the average speed over multiple GeoST segments from the A4540 and A38 roads; 85 segments, with 40 on the A38 described in the preceding section, and 45 segments from the A4540 which form part of Birmingham's inner ring road. The selected segments are highlighted in blue in the West Midlands street network shown in Fig. 2(d).

PDFs for the average speed over the considered journeys are shown in Fig. 6, for four time slots on five different days. Morning rush hours, evening rush hours, daytime non-rush hours (which are the combination of 'morning non-rush hours' and 'afternoon non-rush hours'), and evening non-rush hours (see Section 2.3) are presented by solid, dashed, dotted, dot-dashed lines and are labelled by Mo_RH, Ev_RH, DNo_RH, and EvNo_RH, respectively. Fig. 6, shows a near bimodal average speed distribution for weekdays, especially during rush hours. Over the weekend, the distribution becomes more unimodal in shape. The weekday bimodal variation is thought to be due to the spatial impact of the city centre which dictates directional congestion as shown in Fig. 5 (a) and (b) for single segments.

During the weekdays, the sharpest peaks in the PDF are observed during the early morning non-rush hours, whereas during the weekend

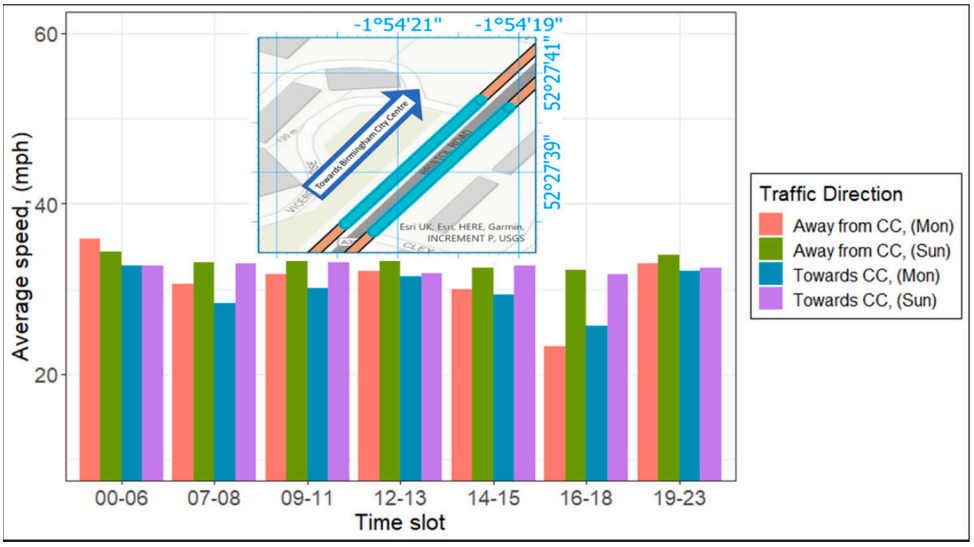

(a)

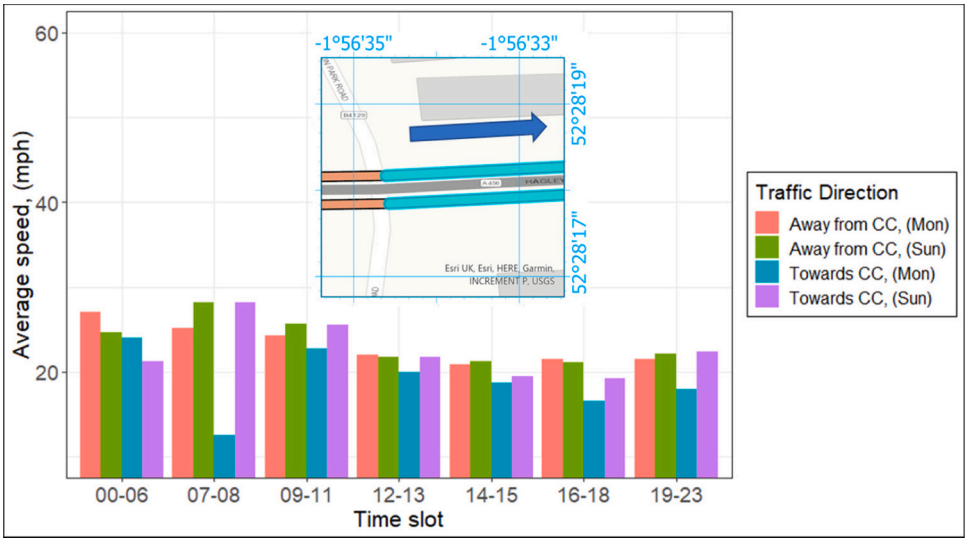

(b)

Fig. 5. The average speed of vehicles moving over (a) a pair of GeoST segments far from the junction and (b) a pair of GeoST segments close to the junction.

days the sharpest peaks are during the morning rush hours (as defined for the working day). The differences between the weekend and weekday days are interesting and potentially highlight that average speed reflects both congestion and driving behaviour.

The shape of the distribution of the theoretical journey shown in this section shows that the combination of individual segments, discussed in Section 4.3, leads to complex flow behaviour throughout the urban road network, which can be captured and explored with the telematics approach detailed in this paper.

4.5. Travel characteristics (average vehicle speed) for the West Midlands region

In this section, we produce average speed PDFs for different road types (secondary roads, primary roads and motorways) over the whole of the West Midlands region for the different time slices, see Fig. 7(a-c). The results for the years 2016 and 2018 are presented by the black dashed and solid lines, respectively. The official speed limits over every road type are represented by vertical red solid lines.

The PDF profiles of the average traffic flow speeds for the primary and secondary roads show near unimodal distribution over all time slices. The unimodal distribution of the average speed profile moves either right (faster) or left (slower) by hours of the day, while the peak height is almost constant. Average peak speeds decrease in rush hours.

Fig. 7(a) also shows a significant contribution of vehicles exceeding the upper-speed limit of 30mph on secondary roads. In non-rush hours, and especially late night and early morning when the roads are emptier, more vehicles exceed the speed limits. A similar analysis is not straightforward for primary roads because the speed limit varies from 30 to 40 mph dependent upon location, as indicated in Fig. 7(b). Nevertheless, if the speed limit of 30 mph is assumed as the upper-speed limit, the percentage of vehicles exceeding the speed limit in non-rush hours is higher than during rush hours.

Fig. 7(c) shows that the PDF profile of the average speed over the motorways is much more variable during a typical day, compared to primary and secondary roads. Whilst the peak of the profile moves toward the higher speed limit of 70 mph during the late night and early morning periods. During the daytime, it peaks closer to 60 mph. During

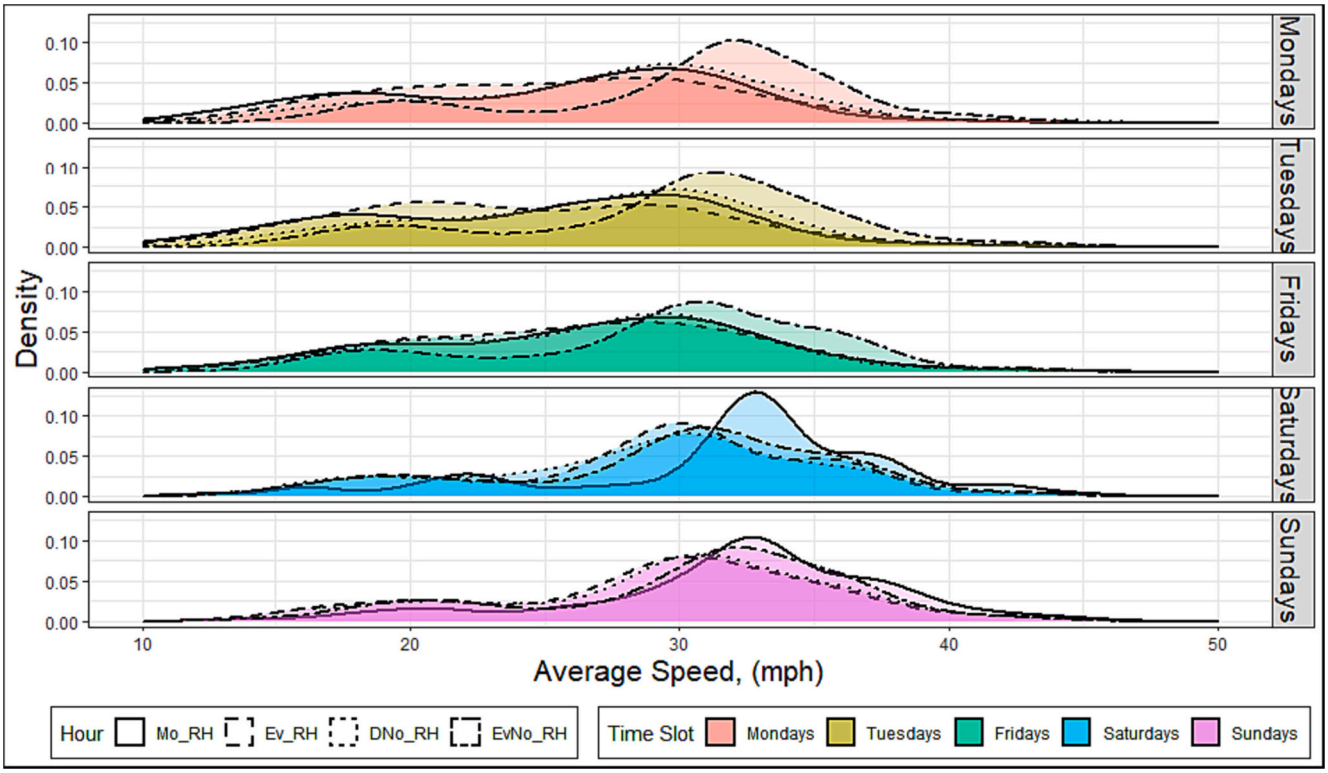

Fig. 6. The average speed of vehicles moving over a set of GeoST segments consisting of 85 road segments of the A38 and A4540 roads which is highlighted in blue in Fig. 2(d). Morning rush hours, evening rush hours, daytime non-rush hours, and evening non-rush hours (see Section 2.3) are presented by solid, dashed, dotted, dot-dashed lines and are labelled by Mo_RH, Ev_RH, DNo_RH, and EvNo_RH, respectively. (For interpretation of the references to colour in this figure legend, the reader is referred to the web version of this article.)

rush hours, the average speed is much lower compared to the other time slices.

The motorway PDFs show major differences between the 2016 and 2018 data, whereas the secondary and primary road data were more similar between the two study years. The average speed of vehicles on the motorways in 2016 was higher than that of 2018. A total assessment of the results shows that the vehicles in 2016 were on average 1.4%, 1.2%, and 6.4% faster than that in 2018 over secondary roads, primary roads, and motorways, respectively. Whilst the results of the current study show a 3% decrease in the average speed over all the studied roads from 2016 to 2018, the statistics from the UK Department for Transport (DfT) show a 2.4% increase in the number of licenced vehicles in the UK from 37.3 M in 2016 to 38.2 M in 2018 (DFT, 2017, 2019). This suggests a correlation between the average vehicle speed over the road network and the fleet population. The bigger observed differences for the motorways are more interesting and suggest there were major structural differences during the two time periods, and this will be investigated further in future work.

The percentage of segments with average speeds exceeding the speed limit (% segment in excess) is estimated for different hours, days and roads, and is graphically shown in Fig. 7(d). The values here were estimated using the corresponding local speed limits, please see Section 2.5. The percentage of speed limit exceedance in non-rush hours and weekends, when the traffic is lighter, is higher than that of the other time slots. Moreover, the percentage of speed limit exceedance on motorways is significantly smaller than that on secondary or primary roads. This might be due to the higher number of motorway speed cameras compared to the other roads. On average, vehicles exceed the speed limits by 30.4% more at weekends when compared to weekdays.

The PDFs of the average vehicle speed on different days of a week and three example time slots of: afternoon non-rush hours (14:00–15:59), morning rush hours (07:00–08:59), and evening rush hours (16:00–18:59) for years 2016 and 2018 are shown in Fig. 8(a) and (b), respectively. The peak of the profiles moves toward higher speeds at the weekend, in addition to the peak height increasing. For primary and secondary roads, there are surprisingly few differences between the weekday PDFs for the three different diurnal time slices investigated. For motorways, there are clear differences. For Saturdays and Sundays, the morning rush hour period is on average faster than the two other investigated time slices. The day-of-the-week behaviour for 2016 and 2018 is largely similar between the two datasets.

4.6. *Vehicle specific power (VSP)*

VSP over the roads is estimated using the corresponding speed-acceleration-variation profile and the approach proposed here translates the vehicle telematics data into the road VSP with high spatial and temporal resolutions, see Section 2.2. The PDFs of VSP for the studied road types and time slots in the years 2016 and 2018 are presented in Fig. 9. It is noted that we are studying the VSP of light-duty vehicles moving over the West Midlands roads and the calculations reflect these assumptions. The black solid and red dashed lines represent calculated VSP when the road slope is considered or ignored, respectively; see Eq. (5). For most time slices, the VSP PDFs appear to have near normal distributions for the secondary and primary roads. The PDF peaks move to higher VSP values during non-rush hour periods, and to lower VSP values during rush hour periods. The impact of the time of travel upon the peak VSP value is small. The motorway PDFs are more skewed than the primary and secondary roads. The early morning (0:00–6:59) PDFs show a secondary peak with negative VSP, which likely indicates more aggressive driving occurring during these hours.

Fig. 9 shows that ignoring road slope causes distinct differences in the calculated VSPs. When averaged over the whole year and all segments, the average impact of including the road slope when calculating

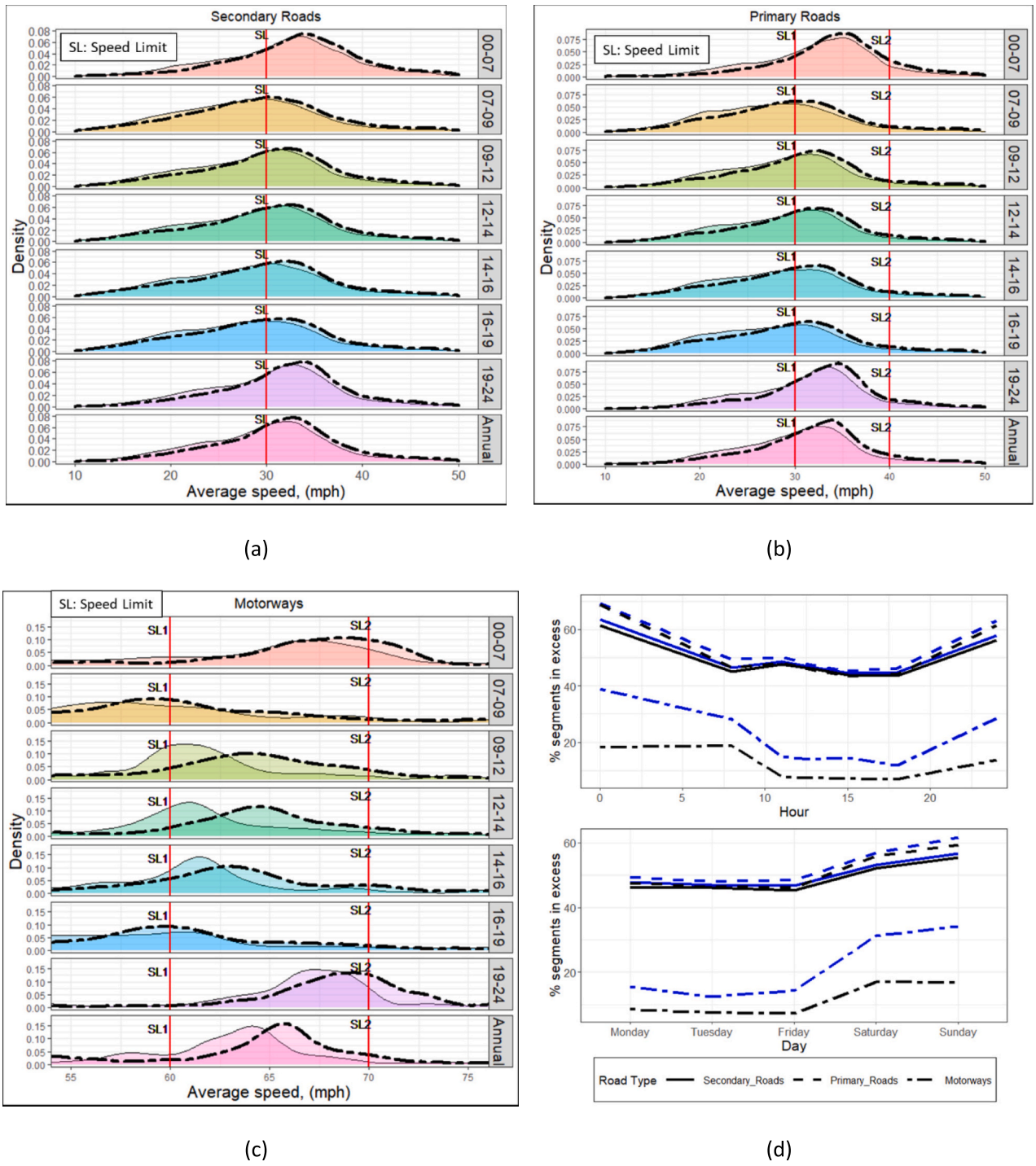

Fig. 7. The probability distribution function (PDF) of the vehicles (traffic flow) speeds over (a) secondary roads, (b) primary roads, and (c) motorways of West Midlands; (d) percentage of segments in exceedance of the local speed limit (% segments in excess) for the different times and roads, see Eq. 8. In Fig. 6(a) – 6(c), black dashed and solid lines are for the results of 2016 and 2018, respectively, and the vertical solid red lines stand for official speed limits over the studied roads. In Fig. 6(d), black and blue colours represent the results for the years 2016 and 2018, respectively. (For interpretation of the references to colour in this figure legend, the reader is referred to the web version of this article.)

VSP, is to decrease the VSP by 12.7%, 14.3%, and 12.6% for driving over secondary roads, primary roads, and motorways, respectively. The observed VSP profiles for the 2016 and 2018 years are very similar.

Fig. 10 shows the VSP PDFs for the morning rush hour, evening rush hours and afternoon non-rush hour periods for the different days of the week. The VSPs are also estimated with or without road slope, respectively. The weekday PDFs are approximately normal distributed for all road types. However, the weekend distributions have an additional peak around the zero VSP value, while the main peak of the profile is dampened compared to the weekdays. One of the interesting aspects of Fig. 10 is the cruise driving peak which is formed around the zero VSP value. It was formed through the morning rush hours and by moving toward the weekends, whereby Sunday's peak is higher than Saturday's one. This might be attributed to the road occupancy level then; roads are usually emptier on Sunday morning than the other times of the week.

VSP is a very useful metric for the study of vehicle emissions and fuel

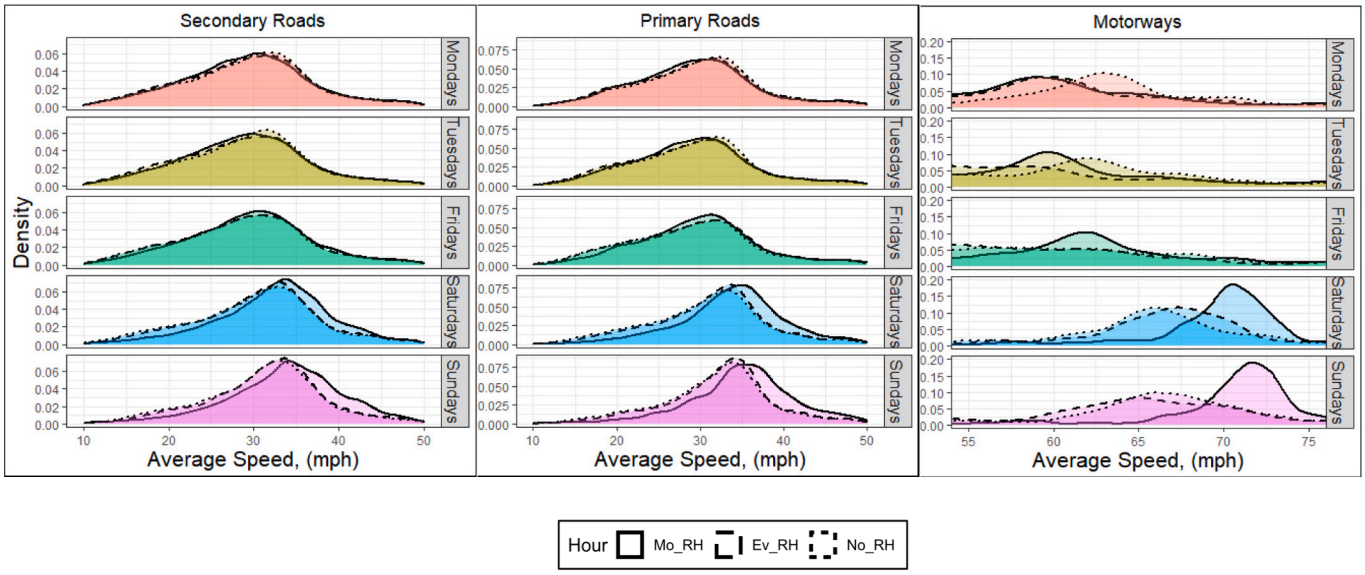

(a)

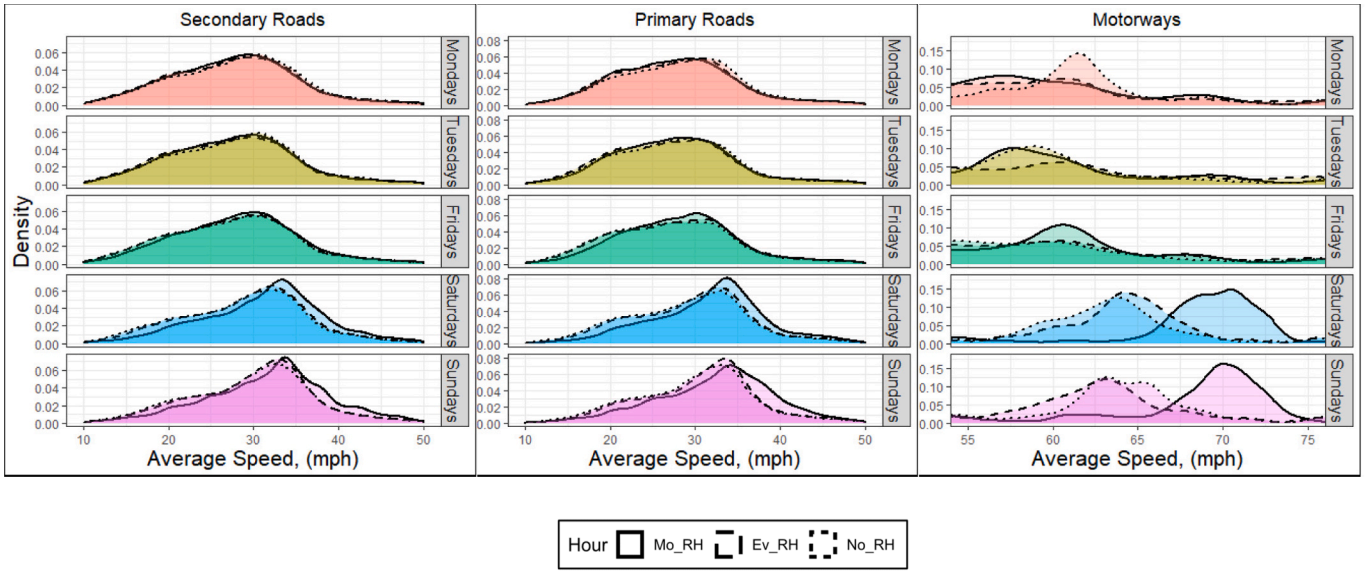

(b)

Fig. 8. The probability distribution function (PDF) of the vehicles (traffic flow) speeds over secondary roads, primary roads, and motorways for morning rush hours (Mo_RH), evening rush hours (Ev_RH), non-rush hours (No_RH) for the years (a) 2016 and (b) 2018. Mo_RH, Ev_RH, and No_RH stand here for the hours 7–8, 16–18, and 14–15, respectively.

consumption over the roads. With this telematics-derived VSP dataset, the corresponding emission factors as well as fuel consumption can be now calculated in future work.

5. Conclusions and future research direction

With the pace of advancements in telecommunication technologies, the access of civilians to global navigation satellite systems and hence the increasing number of connected vehicles moving within urban areas, telematics data has great potential for revolutionizing our understanding of vehicle flow. This paper provides a new approach to translating telematics data into useful parameterizations of urban mobility and travel characteristics. The approach, GeoST mapping of urban mobility, translates raw instantaneous speed-time data into multiple dimensions of urban mobility over highly detailed spatiotemporal frameworks.

We have demonstrated that the GeoST approach can give detailed maps of vehicle flow over wide areas using data from the West Midlands area, which contains 4.5% of England's road length, over two years: 2016 and 2018. The geospatial data has been subset spatially into different road types: primary roads, secondary roads and motorways. It has also been subset into different days and diurnal time slices to be able to investigate the role of rush hours and other temporal features. From the maps, hot spot analysis can be conducted to locate areas with interesting features.

The unparalleled depth of data makes quality checking of the data complex because there are no comparable real-world measurements to

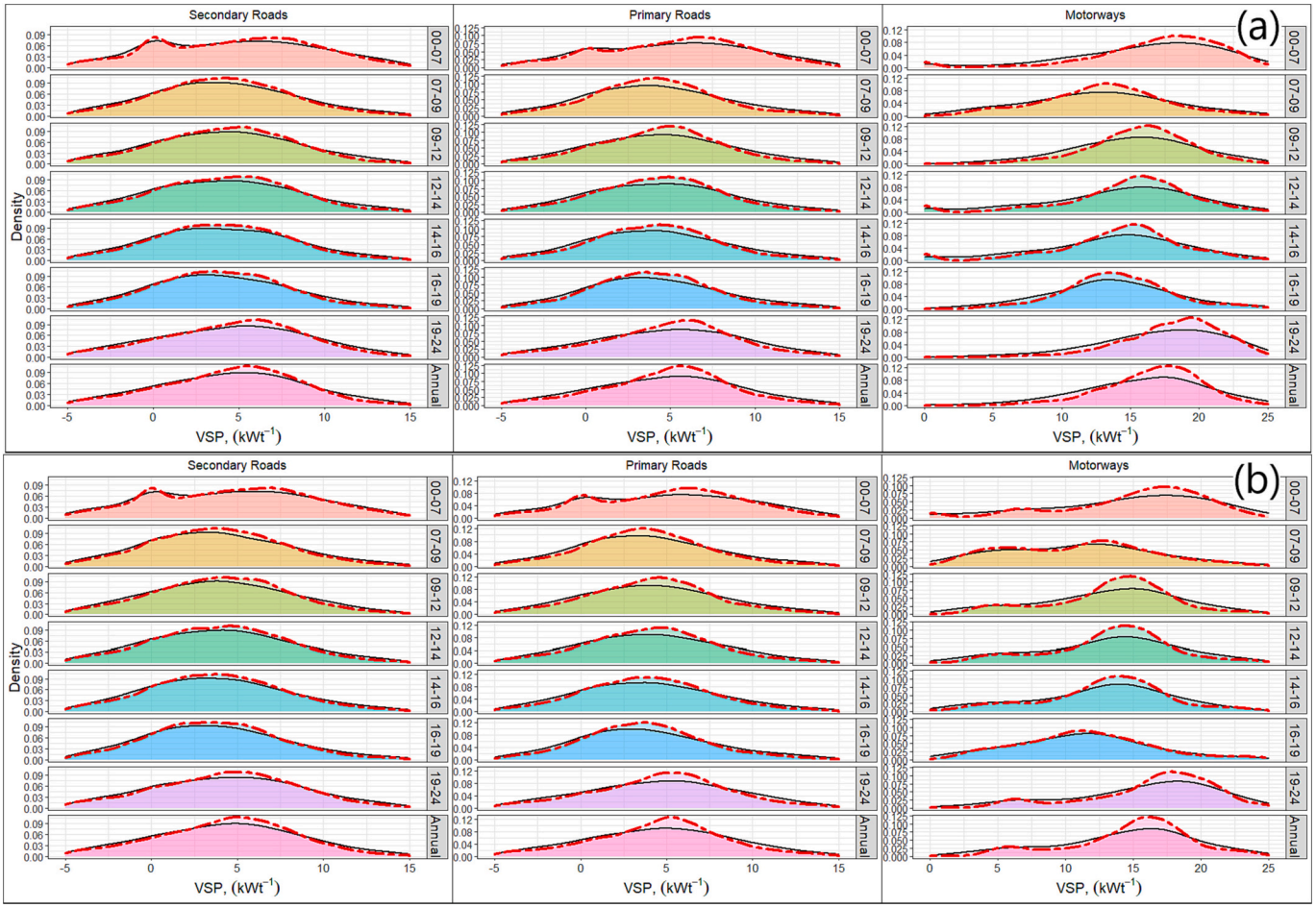

Fig. 9. The probability distribution function (PDF) of vehicular specific power (VSP) for vehicles moving over secondary roads, primary roads, and motorways of West Midlands in different time slots of the years (a) 2016 and (b) 2018. Black solid and red dashed lines stand for with and without considering the role of road slope in calculating the VSP (see Eq. (5)), respectively. (For interpretation of the references to colour in this figure legend, the reader is referred to the web version of this article.)

compare against. When compared to modelled data from the local regional transportation organization (TfWM), which are generated for similar but non-identical conditions, a difference of ~5.1 mph is observed between the measured average speed and the modelled data.

The GeoST approach is demonstrated at different scales. Data for two individual road segments, both approximately 150 m long are used to highlight the microfeatures of traffic behaviour that can be derived from telematics data. The derived data show how the presence of geospatial features such as junctions can affect traffic flow. By combining 85 road segments a theoretical journey is demonstrated and additional complexity in the speed distributions, as compared to individual segments, is shown. Using the whole West Midlands dataset, differences in average speeds, travel times, and VSPs are shown throughout the study area. For example, it is shown that vehicle flow speeds were on average faster in 2016 compared to 2018 for the whole West Midlands region.

The methodology calculates VSP with and without the inclusion of road slope into the VSP calculation. The inclusion of realistic road slope parameterizations changes the derived VSP over the whole of the West Midlands by ~12–14%. The new methodology is also used to demonstrate and parameterize adherence to speed limit regulations. For example, on average, vehicles exceed the speed limits by 30.4% more at weekends when compared to weekdays.

This paper demonstrates that the new approach of GeoST mapping, using telematics as input data, provides excellent opportunities for understanding urban mobility and opens new windows for transport planning and environmental research.

Going forwards, the new GeoST approach provides a new tool for improving our understanding of urban mobility and will be of great benefit to multiple stakeholders. With the increasing availability of telematics data, the approach described can be extended to further locations worldwide.

The proposed approach visualises urban mobility over geospatial frameworks with fine resolutions. This enables the parametrization and discussion of the impact of other urban features, such as schools, hospitals, and car parks, on urban mobility. The approach also provides a foundation for advanced technologies, such as the Internet of Things (IoT) and Vehicle-to-Vehicle (V2V) or Vehicle-to-Road (V2R) communication. Furthermore, this approach can be seen as a progression toward digitally constructed environments, including digital twins. The suggested method provides temporal attribution for digitally constructed transportation. Smart algorithms can be trained using spatial and temporal variations from previous years to predict the future of road transport. This is a promising avenue for future research.

CRediT authorship contribution statement

Omid Ghaffarpasand: Conceptualization, Data curation, Formal analysis, Investigation, Methodology, Software, Writing – original draft, Writing – review & editing. **Francis D. Pope:** Conceptualization, Funding acquisition, Investigation, Methodology, Project administration, Writing – review & editing.

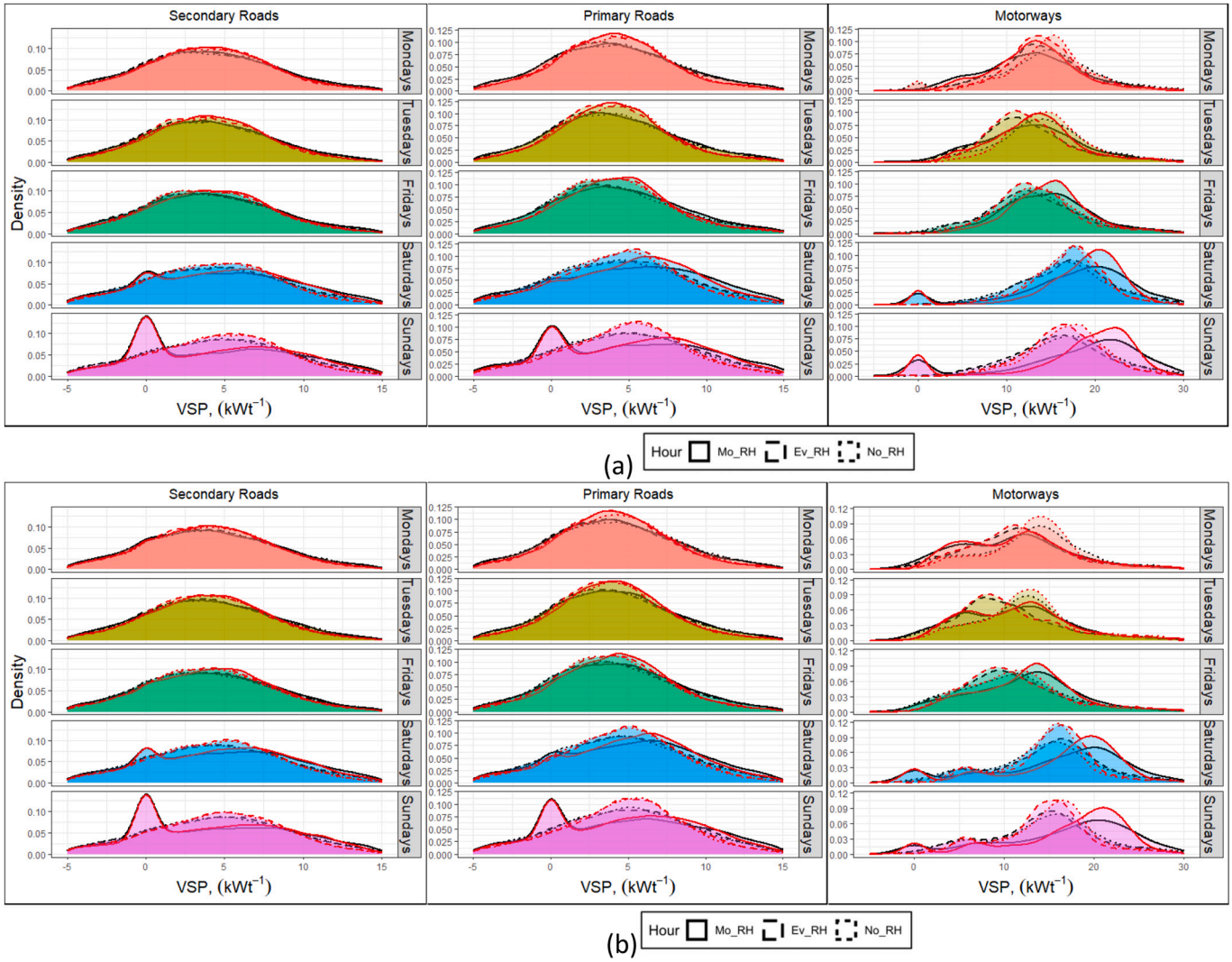

Fig. 10. The probability distribution function (PDF) of vehicular specific power (VSP) for vehicles moving over secondary roads, primary roads, and motorways of West Midlands in different days of the years (a) 2016 and (b) 2018. Black solid and red dashed lines stand for with and without considering the role of road slope in calculating the VSP (see Eq. (5)), respectively. Mo_RH, Ev_RH, and No_RH stand here for the hours 7–8, 16–18, and 14–15, respectively. (For interpretation of the references to colour in this figure legend, the reader is referred to the web version of this article.)

Declaration of competing interest

The authors declare that they have no known competing financial interests or personal relationships that could have appeared to influence the work reported in this paper.

Data availability

Data will be made available on request.

Acknowledgements

We gratefully acknowledge the support and funding from the Natural Environment Research Council, UK (NERC) via the WM-Air (NE/S003487/1) and TRANSITION Clean Air Network (NE/V002449/1), and the Met Office via the SPF Clean Air Program funding of the DUKEMS Project.

References

Administration, F. H, 1998. Synthesis of Safety Research Related to Speed and Speed Limits. U.S. Department of Transportation.
Alrassy, P., Smyth, A.W., Jang, J., 2023. Driver behavior indices from large-scale fleet telematics data as surrogate safety measures. Accid. Anal. Prev. 179, 106879.
Arun, N.H., Mahesh, S., Ramadurai, G., Shiva Nagendra, S.M., 2017. Development of driving cycles for passenger cars and motorcycles in Chennai, India. Sustain. Cities Soc. 32, 508–512.
Bahrami, Mojtaba, Marek, Ziebart, 2010. Instantaneous Doppler-aided RTK positioning with single frequency receivers. In: *IEEE/ION Position, Location and Navigation Symposium*. IEEE, pp. 70–78.
BCC, 2017. Birmingham Clean Air Zone Feasibility Study. Birmingham City Council.
Börjesson, M., Bastian, A., Eliasson, J., 2021. The economics of low emission zones. Transp. Res. A Policy Pract. 153, 99–114.
Brannigan, A., Zwerman, W., 2001. The Real "Hawthorne Effect". Springer-Verlag.
Davison, J., Bernard, Y., Borken-Kleefeld, J., Farren, N.J., Hausberger, S., Sjödin, Å., Tate, J.E., Vaughan, A.R., Carslaw, D.C., 2020. Distance-based emission factors from vehicle emission remote sensing measurements. Sci. Total Environ. 739, 139688.
Dey, S., Caulfield, B., Ghosh, B., 2019. Modelling uncertainty of vehicular emissions inventory: A case study of Ireland. J. Clean. Prod. 213, 1115–1126.
DFT, 2013. Setting Local Speed Limits. Department for Transport.
DFT, 2017. Vehicle Licensing Statistics: 2016. Department for Transport.
DFT, 2019. Vehicle Licensing Statistics: 2018. Department for Transport.
DFT, 2020. Road Traffic Statistics. Department for Transport.
DFT, 2022. Road Lengths in Great Britain: 2020. Department for Transport, UK government.
EEA, 2019. Emissions of Air Pollutants from Transport. European Environmnet Agency.
Elvik, R., 2005. Speed and road safety: synthesis of evidence from evaluation studies. Transp. Res. Record J. Transp. Res. Board 1908, 59–69.
Frey, H.C., Zheng, J., 2002. Probabilistic analysis of driving cycle-based highway vehicle emission factors. Environ. Sci. Technol. 36, 5184–5191.

Galgamuwa, U., Perera, L., Bandara, S., 2015. Developing a general methodology for driving cycle construction: comparison of various established driving cycles in the world to propose a general approach. J. Transp. Technol. 5, 191–203.
Gao, G., Meng, S., Wüthrich, M.V., 2022. What can we learn from telematics car driving data: A survey. Insurance Math. Econom. 104, 185–199.
Gately, C.K., Hutyra, L.R., Peterson, S., Sue Wing, I., 2017. Urban emissions hotspots: quantifying vehicle congestion and air pollution using mobile phone GPS data. Environ. Pollut. 229, 496–504.
Ghaffarpasand, Omid, Deo Okure, Green, Paul, Saba Sayyahi, Priscilla, Adong, Sserunjogi, Richard, Engineer Bainomugisha, Francis, D. Pope, 2024. The impact of urban mobility on air pollution in Kampala, an exemplar sub-Saharan African city. Atmospheric Pollution Research 15, 102057.
Ghaffarpasand, O., Pope, F.D., 2023. Telematics data for geospatial and temporal mapping of urban mobility: fuel consumption, and air pollutant and climate-forcing emissions of passenger cars. Sci. Total Environ. 894, 164940.
Ghaffarpasand, O., Talaie, M.R., Ahmadikia, H., Khozani, A.T., Shalamzari, M.D., Majidi, S., 2021a. Real-world evaluation of driving behaviour and emission performance of motorcycle transportation in developing countries: A case study of Isfahan, Iran. Urban Clim. 39, 100923.
Ghaffarpasand, O., Talaie, M.R., Ahmadikia, H., Talaiekhozani, A., Shalamzari, M.D., Majidi, S., 2021b. How does unsustainable urbanization affect driving behavior and vehicular emissions? Evidence from Iran. Sustain. Cities Soc. 72, 103065.
Ghaffarpasand, O., Burke, M., Osei, L.K., Ursell, H., Chapman, S., Pope, F.D., 2022. Vehicle telematics for safer, cleaner and more sustainable urban transport: a review. Sustain. [Online] 14.
Grange, S.K., Farren, N.J., Vaughan, A.R., Rose, R.A., Carslaw, D.C., 2019. Strong temperature dependence for light-duty diesel vehicle NOx emissions. Environ. Sci. Technol. 53, 6587–6596.
Huang, Y., Meng, S., 2019. Automobile insurance classification ratemaking based on telematics driving data. Decis. Support. Syst. 127, 113156.
Huertas, J.I., Giraldo, M., Quirama, L.F., Díaz, J., 2018. Driving cycles based on fuel consumption. Energies 11, 3064.
Ibarra-Espinosa, S., Ynoue, R.Y., Ropkins, K., Zhang, X., De Freitas, E.D., 2020. High spatial and temporal resolution vehicular emissions in south-East Brazil with traffic data from real-time GPS and travel demand models. Atmos. Environ. 222, 117136.
IEA, 2020. Transport; Improving the sustainability of passenger and freight transport. International Energy Agency.
Javed, M.A., Zeadally, S., Hamida, E.B., 2019. Data analytics for cooperative intelligent transport systems. Vehicul. Commun. 15, 63–72.
Jimenez-Palacios, J.L., 1998. Understanding and Quantifying Motor Vehicle Emissions with Vehicle Specific Power and TILDAS Remote Sensing. Massachusetts Institute of Technology.
Kioutsioukis, I., Kouridis, C., Gkatzoflias, D., Dilara, P., Ntziachristos, L., 2010. Uncertainty and sensitivity analysis of National Road Transport Inventories Compiled with COPERT 4. Procedia Soc. Behav. Sci. 2, 7690–7691.
Li, H., Graham, D.J., Majumdar, A., 2013. The impacts of speed cameras on road accidents: an application of propensity score matching methods. Accid. Anal. Prev. 60, 148–157.
Lyons, T.J., Kenworthy, J.R., Austin, P.I., Newman, P.W.G., 1986. The development of a driving cycle for fuel consumption and emissions evaluation. Transp. Res. Part A: General 20, 447–462.
Mcfarland, R.A., 1956. Human factors in highway transport safety. SAE Trans. 64, 730–750.
Michon, J.A., Koutstaal, G.A., 1969. An instrumented car for the study of driver behavior. Am. Psychol. 24, 297–300.
Milne, D., Watling, D., 2019. Big data and understanding change in the context of planning transport systems. J. Transp. Geogr. 76, 235–244.
Nam, E., 2009. Drive cycle development and real-world data in the United States. In: Presentation at the United Nations Economic Commission for Europe, WLTP-02-17.
Necula, E., 2015. Analyzing traffic patterns on street segments based on GPS data using R. Transp. Res. Procedia 10, 276–285.
Osei, L.K., Ghaffarpasand, O., Pope, F.D., 2021. *Real-World Contribution of Electrification and Replacement Scenarios to the Fleet Emissions in West Midland Boroughs, UK*. Atmosphere 12. https://doi.org/10.3390/atmos12030332.
Papamichail, I., Bekiaris-Liberis, N., Delis, A.I., Manolis, D., Mountakis, K.-S., Nikolos, I. K., Roncoli, C., Papageorgiou, M., 2019. Motorway traffic flow modelling, estimation and control with vehicle automation and communication systems. Annu. Rev. Control. 48, 325–346.
Pestel, N., Wozny, F., 2021. Health effects of low emission zones: evidence from German hospitals. J. Environ. Econ. Manag. 109, 102512.
Pouresmaeili, M.A., Aghayan, I., Taghizadeh, S.A., 2018. Development of Mashhad driving cycle for passenger car to model vehicle exhaust emissions calibrated using on-board measurements. Sustain. Cities Soc. 36, 12–20.
Tang, J., Liu, F., Wang, Y., Wang, H., 2015. Uncovering urban human mobility from large scale taxi GPS data. Phys. A: Stat. Mechan. Appl. 438, 140–153.
Tong, H.Y., Hung, W.T., 2010. A framework for developing driving cycles with on-road driving data. Transp. Rev. 30, 589–615.
Wu, L., Zhang, R., Zhou, R., Wu, D., 2021. An edge computing based data detection scheme for traffic light at intersections. Comput. Commun. 176, 91–98.
Xiang, Junjun, Omid Ghaffarpasand, Francis, D. Pope, 2024. Mapping urban mobility using vehicle telematics to understand driving behaviour. Scientific Reports 14, 3271.
Yuhui, P., Yuan, Z., Huibao, Y., 2019. Development of a representative driving cycle for urban buses based on the K-means cluster method. Clust. Comput. 22, 6871–6880.
Zhai, G., Xie, K., Yang, D., Yang, H., 2022. Assessing the safety effectiveness of citywide speed limit reduction: A causal inference approach integrating propensity score matching and spatial difference-in-differences. Transp. Res. A Policy Pract. 157, 94–106.
Ziakopoulos, A., Petraki, V., Kontaxi, A., Yannis, G., 2022. The transformation of the insurance industry and road safety by driver safety behaviour telematics. Case Stud. Transp. Policy 10, 2271–2279.